nature medicine

Treatment of cerebral ischemia by disrupting ischemia-induced interaction of nNOS with PSD-95

Li Zhou[1,5], Fei Li[2,5], Hai-Bing Xu[1,5], Chun-Xia Luo[1,3], Hai-Yin Wu[1,3], Ming-Mei Zhu[1], Wei Lu[4], Xing Ji[2], Qi-Gang Zhou[1,3] & Dong-Ya Zhu[1,3]

Stroke is a major public health problem leading to high rates of death and disability in adults[1,2]. Excessive stimulation of *N*-methyl-D-aspartate receptors (NMDARs) and the resulting neuronal nitric oxide synthase (nNOS) activation are crucial for neuronal injury after stroke insult[3–7]. However, directly inhibiting NMDARs or nNOS can cause severe side effects because they have key physiological functions in the CNS[5,8–12]. Here we show that cerebral ischemia induces the interaction of nNOS with postsynaptic density protein-95 (PSD-95). Disrupting nNOS–PSD-95 interaction via overexpressing the N-terminal amino acid residues 1–133 of nNOS (nNOS-$N_{1–133}$) prevented glutamate-induced excitotoxicity and cerebral ischemic damage. Given the mechanism of nNOS–PSD-95 interaction, we developed a series of compounds and discovered a small-molecular inhibitor of the nNOS-PSD-95 interaction, ZL006. This drug blocked the ischemia-induced nNOS–PSD-95 association selectively, had potent neuroprotective activity *in vitro* and ameliorated focal cerebral ischemic damage in mice and rats subjected to middle cerebral artery occlusion (MCAO) and reperfusion. Moreover, it readily crossed the blood-brain barrier, did not inhibit NMDAR function, catalytic activity of nNOS or spatial memory, and had no effect on aggressive behaviors. Thus, this new drug may serve as a treatment for stroke, perhaps without major side effects.

PSD-95 is a scaffolding protein that binds both NMDARs and nNOS at excitatory synapses and assembles them into a macromolecular signaling complex[13,14]. Activation of nNOS depends on its association with PSD-95 and on NMDAR-mediated calcium influx[6]. It is known that nNOS contributes to glutamate-induced neuronal death[7]. Brain nNOS exists in particulate and soluble forms[15] and is distributed mainly in the cytosol[16]. nNOS is targeted to membranes by binding to syntrophin, PSD-95, PSD-93 or synapse-associated protein-90 (ref. 17). Neurons lacking PSD-95 or nNOS show reduced excitotoxic vulnerability[18]. Notably, the solubility of nNOS is decreased after ischemia[19]. As membrane-associated protein complexes are generally insoluble[20], we wondered whether ischemia-induced neuronal death is caused by NMDAR-dependent nNOS translocation from cytosol to membrane via nNOS–PSD-95 interaction. If so, disrupting the ischemia-induced nNOS–PSD-95 interaction may be a strategy to treat stroke that not only prevents ischemic damage but also avoids the undesirable effects of directly blocking NMDAR function and inhibiting nNOS activity.

To address this hypothesis (**Fig. 1a**), we performed coimmunoprecipitation experiments with the ipsilateral cortices of mice subjected to MCAO and 24-h reperfusion. Ischemia caused a significant increase in nNOS–PSD-95 complex (**Fig. 1b**). To determine whether the nNOS–PSD-95 interaction is related to NMDAR activation, we treated cultured neurons with glutamate and glycine (Glu-Gly). Reciprocal coimmunoprecipitations showed that the treatment promoted nNOS–PSD-95 interaction (**Fig. 1c**,**d**). The increase in the nNOS–PSD-95 complex was not due to nNOS overexpression because ischemia reduced nNOS expression (**Fig. 1e**). Moreover, the NMDAR-2B (NR2B)-specific antagonist Ro25-6981 or Tat-NR2B9c, a peptide that uncouples PSD-95 and NR2B (ref. 13), decreased the amount of nNOS–PSD-95 complex in the cultured neurons treated with Glu-Gly (**Supplementary Fig. 1**), suggesting a role for NMDAR-dependent signaling in inducing nNOS–PSD-95 interaction.

To explore whether NMDAR activation provokes nNOS translocation from cytosol to membrane, we examined nNOS amounts in the membrane and cytosol fractions of cultured neurons treated with Glu-Gly. The treatment increased nNOS abundance in the membrane fraction (**Fig. 1f**), decreased nNOS abundance in the cytosol fraction (**Fig. 1g**), had no effect on total amounts of nNOS (nNOS / β-actin: 0.769 ± 0.051 (Mg^{2+}-free Locke's buffer) versus 0.777 ± 0.75 (Glu-Gly), $n = 3$, $P > 0.05$) and enhanced nNOS immunofluorescence intensity in the membrane of neurons (**Fig. 1h**). The nNOS translocation may have a key role in cerebral ischemia because nNOS was necessary for NMDAR-dependent neuronal death (**Supplementary Fig. 2**).

To examine whether disrupting the nNOS–PSD-95 interaction prevents cerebral ischemic injury, we generated a lentiviral vector that selectively expresses nNOS-$N_{1–133}$, a region crucial for nNOS–PSD-95 interaction[21,22], and named it LV-nNOS-$N_{1–133}$-GFP. LV-nNOS-$N_{1–133}$-GFP effectively infected neurons and produced considerable nNOS-$N_{1–133}$ peptides *in vitro* (infection efficiency: ~82%) (**Fig. 2a**,**b**) and in the cortex of C57BL/6 mice (**Fig. 2c**,**d**). Coimmunoprecipitation

[1]Department of Pharmacology, School of Pharmacy, Nanjing Medical University, Nanjing, China. [2]Department of Medicinal Chemistry, School of Pharmacy, Nanjing Medical University, Nanjing, China. [3]Laboratory of Cerebrovascular Disease, Nanjing Medical University, Nanjing, China. [4]Department of Neurobiology, Nanjing Medical University, Nanjing, China. [5]These authors contributed equally to this work. Correspondence should be addressed to D.-Y.Z. (dyzhu@njmu.edu.cn) or C.-X.L. (chunxialuo@njmu.edu.cn).

Received 13 July; accepted 20 September; published online 21 November 2010; doi:10.1038/nm.2245

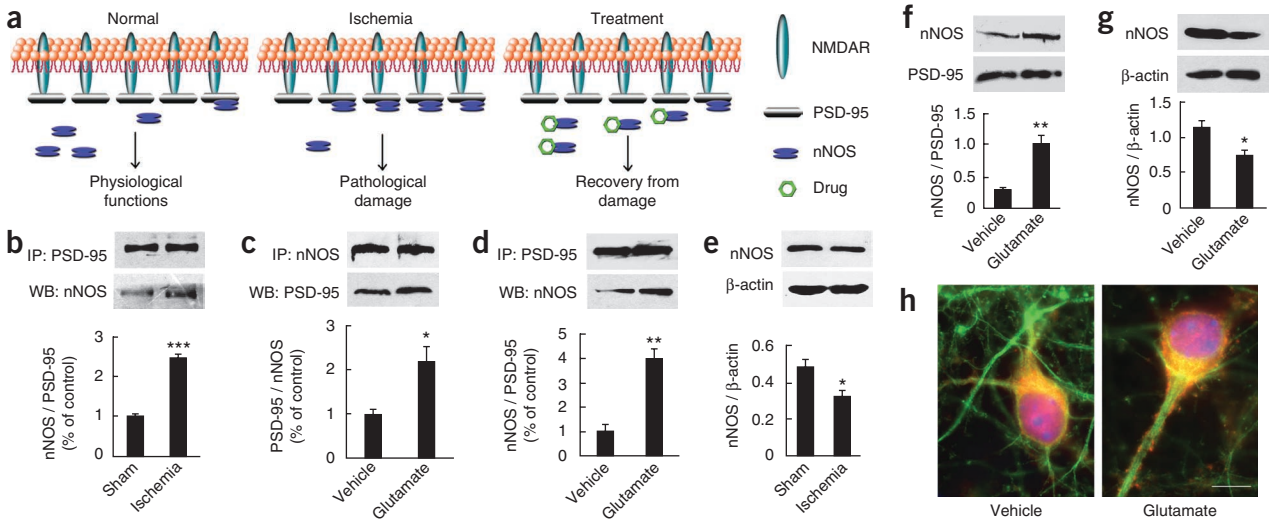

Figure 1 Glutamate-induced nNOS translocation from cytosol to plasma membrane via its binding to PSD-95. (**a**) The hypothesis: cerebral ischemia may induce the translocation of nNOS from cytosol to membrane via nNOS–PSD-95 interaction, and blocking the interaction by drugs may hinder the nNOS translocation, thus reducing ischemic injury following stroke. (**b**–**d**) Coimmunoprecipitation experiments. Samples were immunoprecipitated (IP) and analyzed by western blotting (WB) with the indicated antibodies (top), and the data were quantified (bottom, $n = 3$). (**b**) nNOS–PSD-95 complex amounts in the cortex after ischemia and reperfusion. (**c**,**d**) nNOS–PSD-95 complex amounts in neurons after NMDAR overstimulation, as determined by reciprocal coimmunoprecipitation. (**e**) Immunoblots showing nNOS amounts in the cortex after ischemia and reperfusion (top) and quantification of the data (bottom, $n = 3$). (**f**,**g**) nNOS content in membrane fractions (**f**) and cytosol fractions (**g**) in neurons after NMDAR overstimulation. Representative immunoblots (top) and quantification of these data (bottom, $n = 3$). (**h**) Representative nNOS immunofluorescence in glutamate- and vehicle-treated neurons (red, nNOS; green, β-III-tubulin; blue, Hoechst). Scale bar, 5 μm. Ischemia and reperfusion: mice were subjected to MCAO for 90 min and reperfusion for 30 min. NMDAR overstimulation: cultured cortical neurons were treated with 50 μM glutamate with 10 μM glycine for 30 min. Values are means ± s.e.m., $^{*}P < 0.05$, $^{**}P < 0.01$, $^{***}P < 0.001$, versus sham in **b** and **e** and versus vehicle in **c**, **d**, **f** and **g**.

experiments showed that LV-nNOS-N_{1-133}-GFP significantly decreased the amount of nNOS–PSD-95 complex in cultured neurons treated with Glu-Gly (**Fig. 2e**) and in the ischemic cortex (**Fig. 2f**) and had a weak effect in the nonischemic cortex (**Supplementary Fig. 3a**) at day 5 after infections. Next, we infused LV-nNOS-N_{1-133}-GFP into the right cortex of mice. Five days later, we induced ischemia in the right hemisphere by MCAO and tested neurological outcome and infarct size at 24 and 24.5 h after reperfusion, respectively.

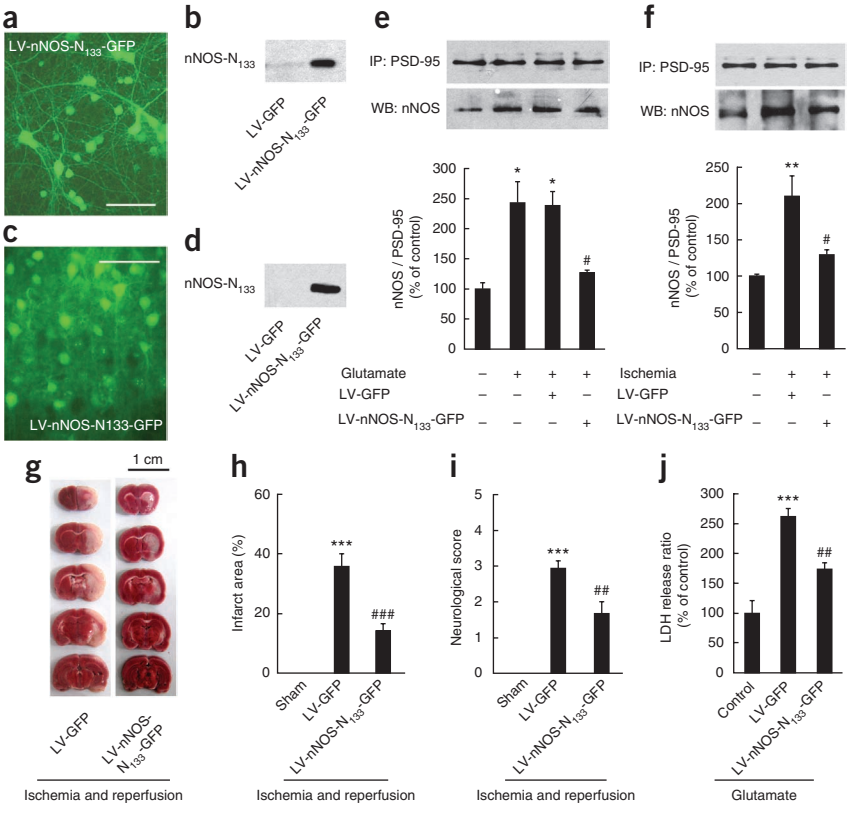

Figure 2 Dissociation of PSD-95–nNOS prevents excitotoxicity and cerebral ischemia. (**a**,**b**) Cultured cortical neurons infected with LV-nNOS-N_{1-133}-GFP vectors expressed nNOS-N_{1-133}. (**a**) A representative fluorescence image. Scale bar, 50 μm. (**b**) Representative immunoblots. (**c**,**d**) The cortices infected with LV-nNOS-N_{1-133}-GFP vectors expressed nNOS-N_{1-133}. (**c**) A representative fluorescence image. Scale bar, 50 μm. (**d**) Representative immunoblots. (**e**,**f**) Coimmunoprecipitation experiments showing the effect of LV-nNOS-N_{1-133}-GFP on nNOS–PSD-95 interaction: samples were immunoprecipitated and analyzed by western blotting with the indicated antibodies (top), and data were analyzed (bottom). (**e**) nNOS–PSD-95 complex amounts in neurons exposed to 50 μM glutamate with 10 μM glycine for 30 min ($n = 3$). (**f**) nNOS–PSD-95 complex amounts in the cortex of mice subjected to 90 min MCAO and 30 min reperfusion ($n = 3$). (**g**) Representative of triphenyltetrazolium chloride–stained brain slices. (**h**,**i**) Effects of LV-nNOS-N_{1-133}-GFP on cerebral ischemia in mice subjected to 90 min MCAO. Infarct size (**h**) and neurological score (**i**) were measured at 24.5 and 24 h after reperfusion ($n = 8$). (**j**) Effects of LV-nNOS-N_{1-133}-GFP on lactate dehydrogenase (LDH) release from cultured cortical neurons exposed to 50 μM glutamate with 10 μM glycine for 30 min ($n = 5$). Values are means ± s.e.m., $^{*}P < 0.05$, $^{**}P < 0.01$, $^{***}P < 0.001$, versus control in **e**, **f** and **j** and versus sham in **h** and **i**; $^{\#}P < 0.05$, $^{\#\#}P < 0.01$, $^{\#\#\#}P < 0.001$, versus LV-GFP.

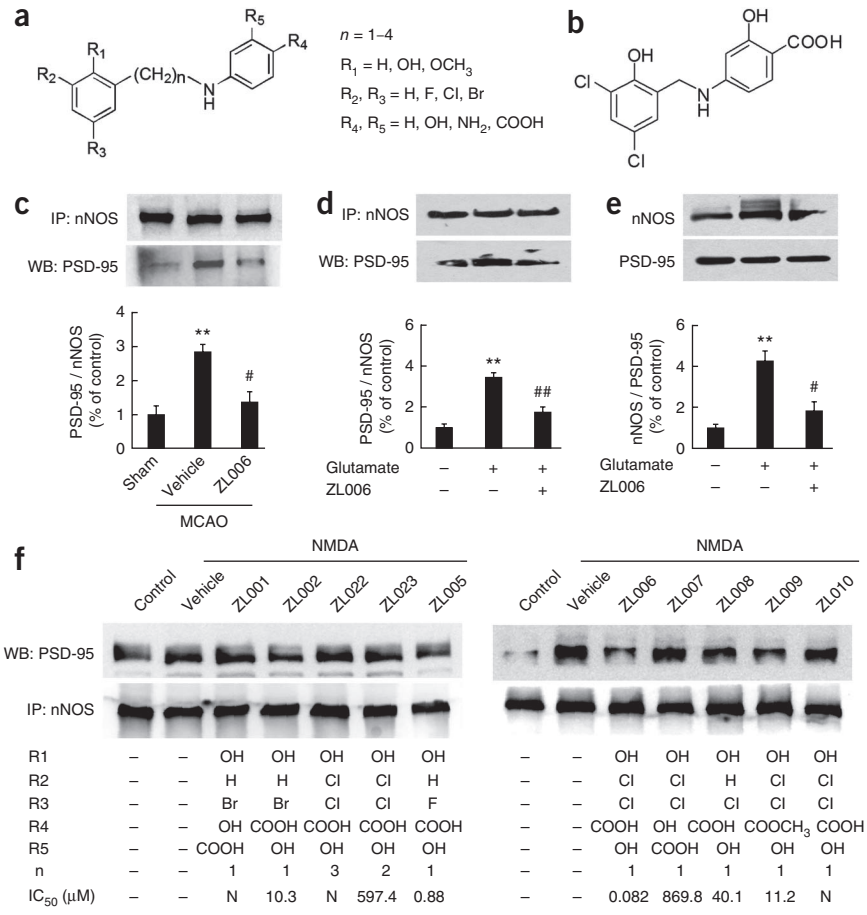

Figure 3 Effects of target compounds on nNOS–PSD-95 interaction. (**a**) Structures of target compounds. *n* indicates the number of CH_2. (**b**) Structure of ZL006. (**c**,**d**) Coimmunoprecipitation experiments showing the effect of ZL006 on nNOS–PSD-95 interaction. Samples were immunoprecipitated and analyzed by western blotting with the indicated antibodies (top), and the data were analyzed (bottom). (**c**) nNOS–PSD-95 complex amounts in the cortex of mice subjected to 90 min MCAO and 30 min reperfusion ($n = 3$). (**d**) nNOS–PSD-95 complex amounts in neurons exposed to 50 μM glutamate with 10 μM glycine for 30 min ($n = 3$). (**e**) Effects of ZL006 on nNOS amounts in the membrane fraction of cultured cortical neurons exposed to 50 μM glutamate with 10 μM glycine for 30 min ($n = 3$). (**f**) Structure-activity relationship of representative compounds. IC_{50} of compounds was measured in cultured cortical neurons exposed to 50 μM glutamate with 10 μM glycine for 30 min. N, no effect. Coimmunoprecipitation experiments were performed in organotypic hippocampal slice cultures (OHSCs) exposed to 25 μM NMDA for 24 h (**Supplementary Fig. 13**). Compounds (10 μM) were added 30 min before NMDA exposure. Similar results were observed in each of three experiments. Values are means ± s.e.m., $^{**}P < 0.01$ versus sham in **c** and versus control in **d** and **e**; $^{\#}P < 0.05$, $^{\#\#}P < 0.01$ versus vehicle in **c** and versus glutamate in **d** and **e**.

LV-nNOS-$N_{1–133}$-GFP treatment significantly decreased infarct size (**Fig. 2g**,**h**) and neurological deficit (**Fig. 2i**). The mortality was 6/14 and 2/10 mice for LV-GFP control and LV-nNOS-$N_{1–133}$-GFP, respectively, indicating an amelioration of ischemic injury. Moreover, LV-nNOS-$N_{1–133}$-GFP reduced lactate dehydrogenase release from cultured neurons treated with Glu-Gly (**Fig. 2j**).

To develop small molecules suitable for clinically treating stroke by disrupting the ischemia-induced nNOS–PSD-95 interaction, we focused on the mechanism for nNOS–PSD-95 PDZ dimer formation. A salt bridge between Asp62 on the nNOS PDZ domain and Arg121 on the nNOS β-finger domain is structurally required for the nNOS β-finger, which interacts with PSD-95. Disruption of this intra-nNOS salt bridge melts down the β-finger structure and prevents its interaction with PSD-95. Moreover, residues Leu107 to Phe111 on the β-finger are crucial for conformational changes induced by its binding to PSD-95 PDZ2 (ref. 22). We thus designed and synthesized a series of compounds with a hydrophobic ring A and a hydrophilic ring B with a carboxyl group. To enhance their flexibility, we designed a linker connecting rings A and B (**Fig. 3a**). These compounds may bind the β-finger via forming an ionic bond between their carboxyl group and the amino group in Arg121 and forming a hydrophobic bond between their ring A and Leu107 or Phe111, thus hindering the conformational change of nNOS PDZ.

We obtained several compounds that prevented glutamate-induced excitotoxicity *in vitro*. Among them, [5-(3,5-dichloro-2-hydroxybenzylamino)-2-hydroxybenzoic acid], which we named ZL006 (**Fig. 3b**), was the most potent. Its structure was confirmed by ^{1}H nuclear magnetic resonance, ^{13}C nuclear magnetic resonance, mass spectrometry and infrared spectra (**Supplementary Table 1**). Coimmunoprecipitation experiments with the cortices of mice subjected to MCAO and 24 h reperfusion showed that pretreatment with ZL006 (1.5 mg per kg body weight intravenously (i.v.), 15 min before MCAO) inhibited the ischemia-induced increase in nNOS–PSD-95 complex (**Fig. 3c**). Moreover, ZL006 significantly reduced nNOS–PSD-95 complex (**Fig. 3d**) and membranous nNOS abundance (**Fig. 3e**) in neurons treated with Glu-Gly. ZL006 had a weak effect on nNOS–PSD-95 interaction (**Supplementary Fig. 3b**) and did not change nNOS expression (nNOS / β-actin: 0.961 ± 0.133 (vehicle) versus 1.051 ± 0.133 (ZL006), $n = 3$, $P > 0.05$) in nonischemic cortex. These findings suggest that ZL006 disrupts the nNOS–PSD-95 interaction *in vitro* and *in vivo*.

To examine whether ZL006 is specific for nNOS–PSD-95, we investigated its effects on nNOS–C-terminal PDZ domain ligand of nNOS, PSD-95–synaptic Ras GTPase–activating protein-1 and NR2B–PSD-95 interactions in the ischemic cortices. The drug did not affect these PDZ-mediated protein-protein interactions (**Supplementary Fig. 4a–c**). Moreover, disruption of the glutamate-induced nNOS–PSD-95 binding by ZL006 cannot be explained by its targeting of AMPA-type glutamate receptors because the AMPA receptor antagonist CNQX had a very weak effect on nNOS–PSD-95 interaction and did not potentiate the effect of ZL006 (**Supplementary Fig. 4d**).

To establish the structure-activity relationship of the compounds we screened, we measured their effects on NMDA-induced lactate dehydrogenase release and nNOS–PSD-95 interaction. The half-maximal inhibitory concentration (IC_{50}) values of these compounds were in accordance with their effects on NMDA-induced nNOS–PSD-95 binding (**Fig. 3f**). The carboxyl group at R_4, the hydroxyl group at R_1 and the length of linker between rings A and B were crucial for their activities.

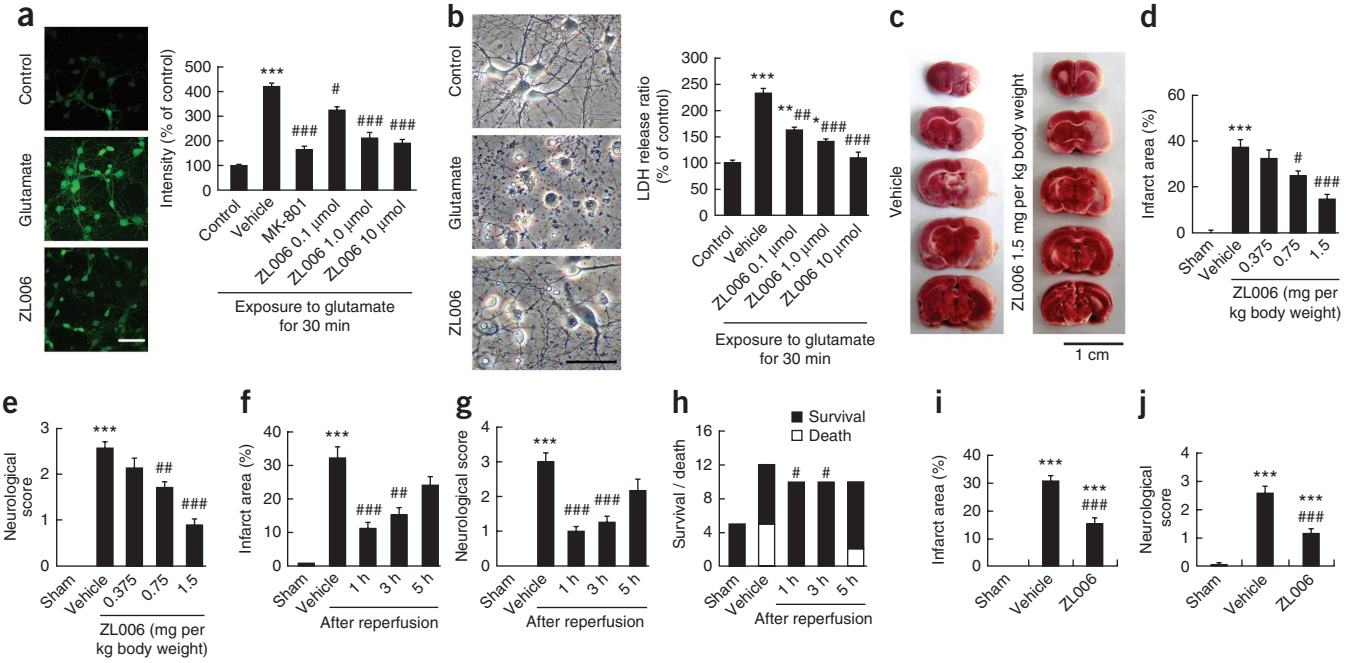

Figure 4 ZL006 prevents NMDAR-dependent excitotoxicity and cerebral ischemia. (**a**) NO synthesis in cultured neurons exposed to 50 μM glutamate with 10 μM glycine for 30 min. Imaging of NO synthesis (left) and summarized data (right, $n = 3$). Scale bar, 40 μm. (**b**) Lactate dehydrogenase release from cultured neurons exposed to 50 μM glutamate with 10 μM glycine for 30 min. Morphological changes of neurons (left) and summarized data (right, $n = 3$). Scale bar = 60 μm. (**c**–**h**) Effects of ZL006 on cerebral ischemia in mice subjected to 90 min MCAO and reperfusion. Neurological score and infarct size were measured at 24 and 24.5 h, respectively, after reperfusion. (**c**) Representative of triphenyltetrazolium chloride–stained slices. (**d**,**e**) Dose-effect relationship experiments ($n = 7$–9). ZL006 or vehicle was administrated at 1 h after reperfusion. (**d**) Infarct size. (**e**) Neurological score. (**f**–**h**) Therapeutic window experiments ($n = 8$–10). Vehicle was given at 1 h after reperfusion. (**f**) Infarct size. (**g**) Neurological score. (**h**) Mortality. (**i**,**j**) Effects of ZL006 on cerebral ischemia in rats subjected to 120 min MCAO and 96 h reperfusion. ZL006 or vehicle was administered 1 h after reperfusion ($n = 8$–11). (**i**) Infarct size. (**j**) Neurological score. Values are means ± s.e.m., $^{*}P < 0.05$, $^{**}P < 0.01$, $^{***}P < 0.001$ versus control in **a** and **b** and versus sham in **d**–**j**; $^{\#}P < 0.05$, $^{\#\#}P < 0.01$, $^{\#\#\#}P < 0.001$ versus vehicle.

We next investigated the effect of ZL006 on nitric oxide (NO) synthesis and lactate dehydrogenase release in cultured neurons treated with Glu-Gly. ZL006 inhibited NMDAR-dependent NO synthesis in a concentration-dependent manner (**Fig. 4a**) and inhibited lactate dehydrogenase release with an IC_{50} of 8.2×10^{-8} M, and it also ameliorated morphological changes (**Fig. 4b**), suggesting a neuroprotective effect. To examine whether ZL006 has benefits in cerebral ischemia, we treated MCAO mice with ZL006 (i.v.) at 1 h after reperfusion and tested neurological outcome and infarct size at 24 and 24.5 h after reperfusion, respectively. ZL006 reduced infarct size (**Fig. 4c**,**d**) and neurological deficit (**Fig. 4e**) in a dose-dependent manner. The mortality was 3/10, 3/10, 2/10 and 1/10 mice for vehicle and 0.375, 0.75 and 1.5 mg per kg body weight ZL006, respectively. To examine the therapeutic window, we treated MCAO mice with ZL006 (1.5 mg per kg body weight) at 1, 3 or 5 h after reperfusion. When given at 1 or 3 h, ZL006 reduced infarct size (**Fig. 4f**), neuroscore (**Fig. 4g**) and mortality (**Fig. 4h**). Moreover, ZL006 (1.5 mg per kg body weight, i.v., 1 h after reperfusion) substantially reduced infarct size and neuroscore of rats subjected to 120 min of MCAO and 96 h of reperfusion (**Fig. 4i**,**j**). In normal rats, ZL006 crossed the blood-brain barrier readily and did not change cerebral blood flow, platelet aggregation or bleeding time (**Supplementary Figs. 5**–**7**). In ischemic rats, ZL006 did not change body weight, arterial blood pressure, P_aO_2, P_aCO_2, pH and rectal temperature (**Supplementary Table 2**). In addition, ZL006 did not inhibit NMDAR, excitatory postsynaptic currents and nNOS activity (**Supplementary Figs. 8** and **9**). Because ZL006 was ineffective against NMDAR-dependent lactate dehydrogenase release from cultured *Nos1*$^{-/-}$ neurons (lacking nNOS) and against ischemic injury in *Nos1*$^{-/-}$ mice (**Supplementary Fig. 10a**,**b**), it seems that nNOS is required for its neuroprotective effects. Moreover, ZL006 was ineffective against staurosporine-induced neuronal death in the presence of Ro25-6981, suggesting its specificity for NMDAR-mediated neuronal death (**Supplementary Fig. 10c**).

nNOS inhibition has proved to impair learning and memory[11,12]. Accordingly, we investigated a possible effect of ZL006 on spatial memory in mice. ZL006 did not change the acquisition of a spatial water maze task, although the nNOS inhibitor 7-NI markedly decreased spatial memory (**Supplementary Fig. 11**). Additionally, *Nos1*$^{-/-}$ mice displayed excessive aggressiveness[23]. We thus investigated a possible effect of ZL006 on aggressive behaviors in mice and found no such effect (**Supplementary Fig. 12**).

Despite the ubiquity of PDZ domain-containing proteins, PSD-95 and nNOS above any others are key in NMDAR-dependent excitotoxicity[18]. Ischemia induces translocation of nNOS from the cytosol to the cell membrane. The translocation may place nNOS adjacent to other PSD-95 ligands, such as the NR2 subunit of NMDARs[6], and account for NMDAR-dependent cerebral ischemic injury[24]. Blocking the nNOS translocation by dissociating nNOS and PSD-95 with LV-nNOS-N_{1-133}-GFP or ZL006 ameliorated cerebral ischemic damage in this study.

NMDAR dysfunction is implicated in multiple brain disorders[25,26]. Selective NMDAR antagonists produce severe side effects, including cognitive problems, hallucinations and even coma[10,27,28]. The inhibition of nNOS impairs learning and memory[11,12] and produces aggressive behavior[29]. In humans, abnormal NOS and NO metabolism is implicated in the pathogenesis and pathophysiology of some neuropsychiatric disorders[30]. ZL006 did not inhibit nNOS catalytic

activity and NMDAR function, and it had no effect on aggressive behavior and spatial memory. Thus, this drug may treat stroke without major side effects.

METHODS

Methods and any associated references are available in the online version of the paper at http://www.nature.com/naturemedicine/.

Note: Supplementary information is available on the Nature Medicine website.

ACKNOWLEDGMENTS

This work was supported by grants from the National Natural Science Foundation of China ((30971021, 81030023) (D.-Y.Z.) and (30901550) (C.-X.L.)). We thank X. Jin, Q.-P. Li, C.-C. Cao, H.-H. Zhou, W.-X. Sun, D.-L. Wu, Y. Hu and J. Zhang for technical assistance.

AUTHOR CONTRIBUTIONS

L.Z. contributed to the design of the study and performed the cell culture studies, coimmunoprecipitation, western blotting, imaging of NO synthesis and surgical preparation. F.L. performed the design and synthesis of target compounds. H.-B.X. contributed to coimmunoprecipitation, structure-activity relationship analyses and behavioral analyses. C.-X.L. contributed to the design of the study and performed cell culture and morphological analysis of cortical neurons. H.-Y.W. participated in surgical preparation, infarct volume measurement, neuroscore assessment, physiological parameter determination, platelet aggregation and bleeding time measurements. M.-M.Z. performed behavioral analyses, lentivirus production and stereotaxic injection. W.L. performed electrophysiological experiments. X.J. participated in synthesis of target compounds. Q.-G.Z. participated in western blotting analysis. D.-Y.Z. initiated the project and participated in the design of the studies. All authors contributed to data analysis.

COMPETING FINANCIAL INTERESTS

The authors declare no competing financial interests.

Published online at http://www.nature.com/naturemedicine/.
Reprints and permissions information is available online at http://npg.nature.com/reprintsandpermissions/.

1. Flynn, R.W., MacWalter, R.S. & Doney, A.S. The cost of cerebral ischaemia. *Neuropharmacology* **55**, 250–256 (2008).
2. Gállego, J., Muñoz, R. & Martínez-Vila, E. Emergent cerebrovascular disease risk factor weighting: is transient ischemic attack an imminent threat? *Cerebrovasc. Dis.* **27**Suppl 1, 88–96 (2009).
3. Lee, J.M., Zipfel, G.J. & Choi, D.W. The changing landscape of ischaemic brain injury mechanisms. *Nature* **399**, A7–A14 (1999).
4. Arundine, M. & Tymianski, M. Molecular mechanisms of glutamate-dependent neurodegeneration in ischemia and traumatic brain injury. *Cell. Mol. Life Sci.* **61**, 657–668 (2004).
5. Lipton, S.A. Pathologically activated therapeutics for neuroprotection. *Nat. Rev. Neurosci.* **8**, 803–808 (2007).
6. Sattler, R. *et al.* Specific coupling of NMDA receptor activation to nitric oxide neurotoxicity by PSD-95 protein. *Science* **284**, 1845–1848 (1999).
7. Dawson, V.L., Kizushi, V.M., Huang, P.L., Snyder, S.H. & Dawson, T.M. Resistance to neurotoxicity in cortical cultures from neuronal nitric oxide synthase-deficient mice. *J. Neurosci.* **16**, 2479–2487 (1996).
8. Smith, P.F. Therapeutic *N*-methyl-d-aspartate receptor antagonists: will reality meet expectation? *Curr. Opin. Investig. Drugs* **4**, 826–832 (2003).
9. Muir, K.W. Glutamate-based therapeutic approaches: clinical trials with NMDA antagonists. *Curr. Opin. Pharmacol.* **6**, 53–60 (2006).
10. Lipton, S.A. Paradigm shift in neuroprotection by NMDA receptor blockade: memantine and beyond. *Nat. Rev. Drug Discov.* **5**, 160–170 (2006).
11. Kelley, J.B., Balda, M.A., Anderson, K.L. & Itzhak, Y. Impairments in fear conditioning in mice lacking the nNOS gene. *Learn. Mem.* **16**, 371–378 (2009).
12. Zhou, L. & Zhu, D.Y. Neuronal nitric oxide synthase: structure, subcellular localization, regulation, and clinical implications. *Nitric Oxide* **20**, 223–230 (2009).
13. Aarts, M. *et al.* Treatment of ischemic brain damage by perturbing NMDA receptor–PSD-95 protein interactions. *Science* **298**, 846–850 (2002).
14. Cao, J. *et al.* The PSD95-nNOS interface: a target for inhibition of excitotoxic p38 stress-activated protein kinase activation and cell death. *J. Cell Biol.* **168**, 117–126 (2005).
15. Hecker, M., Mülsch, A. & Busse, R. Subcellular localization and characterization of neuronal nitric oxide synthase. *J. Neurochem.* **62**, 1524–1529 (1994).
16. Rothe, F., Canzler, U. & Wolf, G. Subcellular localization of the neuronal isoform of nitric oxide synthase in the rat brain: a critical evaluation. *Neuroscience* **83**, 259–269 (1998).
17. Brenman, J.E. *et al.* Interaction of nitric oxide synthase with the postsynaptic density protein PSD-95 and α1-syntrophin mediated by PDZ domains. *Cell* **84**, 757–767 (1996).
18. Cui, H. *et al.* PDZ protein interactions underlying NMDA receptor-mediated excitotoxicity and neuroprotection by PSD-95 inhibitors. *J. Neurosci.* **27**, 9901–9915 (2007).
19. Takagi, N., Logan, R., Teves, L., Wallace, M.C. & Gurd, J.W. Altered interaction between PSD-95 and the NMDA receptor following transient global ischemia. *J. Neurochem.* **74**, 169–178 (2000).
20. Cappuccio, J.A. *et al.* Cell-free expression for nanolipoprotein particles: building a high-throughput membrane protein solubility platform. *Methods Mol. Biol.* **498**, 273–296 (2009).
21. Tochio, H., Hung, F., Li, M., Bredt, D.S. & Zhang, M. Solution structure and backbone dynamics of the second PDZ domain of postsynaptic density-95. *J. Mol. Biol.* **295**, 225–237 (2000a).
22. Tochio, H. *et al.* Formation of nNOS/PSD-95 PDZ dimer requires a preformed beta-finger structure from the nNOS PDZ domain. *J. Mol. Biol.* **303**, 359–370 (2000b).
23. Chiavegatto, S. *et al.* Brain serotonin dysfunction accounts for aggression in male mice lacking neuronal nitric oxide synthase. *Proc. Natl. Acad. Sci. USA* **98**, 1277–1281 (2001).
24. Huang, Z. *et al.* Effects of cerebral ischemia in mice deficient in neuronal nitric oxide synthase. *Science* **265**, 1883–1885 (1994).
25. Moghaddam, B. Bringing order to the glutamate chaos in schizophrenia. *Neuron* **40**, 881–884 (2003).
26. Gielen, M., Siegler Retchless, B., Mony, L., Johnson, J.W. & Paoletti, P. Mechanism of differential control of NMDA receptor activity by NR2 subunits. *Nature* **459**, 703–707 (2009).
27. Koroshetz, W.J. & Moskowitz, M.A. Emerging treatments for stroke in humans. *Trends Pharmacol. Sci.* **17**, 227–233 (1996).
28. Kemp, J.A. & McKernan, R.M. NMDA receptor pathways as drug targets. *Nat. Neurosci.* **5**, 1039–1042 (2002).
29. Nelson, R.J. *et al.* Behavioural abnormalities in male mice lacking neuronal nitric oxide synthase. *Nature* **378**, 383–386 (1995).
30. Tanda, K. *et al.* Abnormal social behavior, hyperactivity, impaired remote spatial memory, and increased D1-mediated dopaminergic signaling in neuronal nitric oxide synthase knockout mice. *Mol. Brain* **2**, 19 (2009).

ONLINE METHODS

Animals. The experimental protocol was approved by the Institutional Animal Care and Use Committee of Nanjing Medical University. We made every effort to minimize the number of mice used and their suffering. In this study, we used homozygous nNOS-deficient mice (*Nos1*$^{-/-}$ mice; C57BL/6;129–*Nos1*^{tm1p1h}) and their wild-type littermates of similar genetic background (B6129SF2) (from Jackson Laboratories, and maintained at Model Animal Research Center of Nanjing University), young-adult male (6–7 weeks old) C57/BL/6 mice and Sprague-Dawley rats (9–10 weeks old or 10 days old). We maintained animals at controlled temperature (20 ± 2 °C) and group housed them (12-h light-dark cycle) with access to food and water *ad libitum*.

Cell culture and glutamate treatment. We prepared and maintained primary cultures of cortical neurons from postnatal day 0 C57BL/6 mice, *Nos1*$^{-/-}$ and wild-type mice as described previously[31]. Neurons used were cultured for 7–9 d *in vitro*. To induce NMDAR-dependent excitotoxicity, we briefly rinsed cells in Mg^{2+}-free Locke's buffer (154 mM NaCl, 5.6 mM KCl, 3.6 mM $NaHCO_3$, 1.3 mM $CaCl_2$, 5.6 mM D-glucose and 5 mM HEPES, pH 7.4) and placed them in the same buffer with 50 μM glutamate and 10 μM glycine for 30 min.

Imaging of nitric oxide synthesis by confocal microscopy. NO synthesis in the cortical neurons was visualized with a cell-permeable fluorescent precursor, DAF-FM (4-amino-5-methylamino-2,7-difluorofluorescein) diacetate (Calbiochem). Inside cells, this is hydrolyzed by cytosolic esterases to nonpermeable DAF-FM. In the presence of nitric oxide and oxygen, the relatively nonfluorescent DAF-FM is converted into the highly fluorescent and photostable triazole form, DAF-FM T, whose fluorescence intensity is directly proportional to the NO concentration. The spectra of the adduct of DAF-FM is independent of pH, and the lowest detection limit of NO by this fluorochrome is 3 nM[32].

Membrane protein fraction extraction. We extracted membrane protein fractions of cortical neurons with the Mem-PER Eukaryotic Membrance Protein Extraction Reagent Kit (Pierce) as described previously[33]. The **Supplementary Methods** contain more details.

Surgical preparation, infarct volume measurement and neuroscore assessment. We induced focal cerebral ischemia in mice and rats by MCAO and reperfusion (**Supplementary Fig. 14**) and performed neuroscore assessment and infarct volume measure as described previously[34]. The **Supplementary Methods** contain more details.

Coimmunoprecipitation. Cultured neurons, organotypic hippocampal slice cultures (OHSCs) or the cortices of mice were lysed and centrifuged. We preincubated the supernatant with protein G–Sepharose beads (Sigma-Aldrich) and then centrifuged to obtain the target supernatant. We incubated antibody-conjugated protein G–Sepharose beads with the target supernatant, centrifuged, washed and heated the beads to elute bound proteins and analyzed proteins by immunoblotting. The **Supplementary Methods** contain more details.

Lentivirus production and stereotaxic injection. We amplified the coding sequence of nNOS-$N_{1–133}$ (N-terminal amino acid residues 1–133 of nNOS) by RT-PCR and ligated them into the pGC-FU plasmid (Shanghai GeneChem) to produce pGC-FU-nNOS-$N_{1–133}$. As a control, we also generated a lentiviral vector that expresses GFP alone (LV-GFP). We carried out cortical injection of LV-nNOS-$N_{1–133}$-GFP or LV-GFP with a stereotaxic instrument (World Precision Instruments). At day 5 after injection, we induced focal cerebral ischemia in mice by MCAO and reperfusion and performed neuroscore assessment and infarct volume measurements at 24 and 24.5 h after reperfusion, respectively. The **Supplementary Methods** contain more details.

Synthesis of target compounds. We synthesized ZL006 as follows: we dissolved 3,5-dichloro-2-hydroxybenzaldehyde (3.82 g) or 4-aminosalicylic acid (3.06 g) in 50 ml ethanol (20 mM), mixed them and refluxed for 30 min, and then cooled to room temperature (22–25 °C). We isolated precipitated solid by filtering the reaction mixture and dried it under infrared light. We suspended the intermediate in 50 ml ethanol and added $NaBH_4$ (1.5 g) to the suspension at 0–5 °C. We stirred the mixture for 30 min and refluxed for 30 min. We added H_2O (50 ml) to the reaction mixture to remove residual $NaBH_4$. We adjusted the reaction mixture to pH 3–4 with concentrated hydrochloric acid and then concentrated it to ~50 ml by rotary evaporation and cooled to room temperature. We isolated the solid by filtration and dried it at 50 °C for 8 h to get a pure product ZL006 at 80.2% yield. We synthesized other target compounds by a similar process.

Statistical analyses. Data are presented as means ± s.e.m. The significance of differences was determined by one-way analysis of variance followed by Scheffe's *post hoc* test. When two factors were assessed, the significance of differences was determined by two-way analysis of variance. χ^2 test was used to compare the mortality of animals between groups. Differences were considered significant when $P < 0.05$.

Additional methods. Detailed methodology, including behavioral testing, electrophysiological recordings, morphological analysis of cortical neurons, cell viability assays, western blot analysis, NOS activity assay, preparation and maintenance of OHSCs, ZL006 concentration determination in blood, cerebrospinal fluid and brain tissue, platelet aggregation and bleeding time measures, is described in the **Supplementary Methods**.

31. Lea, P.M., Movsesyan, V.A. & Faden, A.I. Neuroprotective activity of the mGluR5 antagonists MPEP and MTEP against acute excitotoxicity differs and does not reflect actions at mGluR5 receptors. *Br. J. Pharmacol.* **145**, 527–534 (2005).
32. Quintana, E., Hernández, C., Alvarez-Barrientos, A., Esplugues, J.V. & Barrachina, M.D. Synthesis of nitric oxide in postganglionic myenteric neurons during endotoxemia: implications for gastric motor function in rats. *FASEB J.* **18**, 531–533 (2004).
33. Qoronfleh, M.W., Benton, B., Ignacio, R. & Kaboord, B. Selective enrichment of membrane proteins by partition phase separation for proteomic studies. *J. Biomed. Biotechnol.* **2003**, 249–255 (2003).
34. Longa, E.Z., Weinstein, P.R., Carlson, S. & Cummins, R. Reversible middle cerebral artery occlusion without craniectomy in rats. *Stroke* **20**, 84–91 (1989).

doi:10.1038/nm.2245